Bull. ERS, No.13 (1980)

NONLINEAR OSCILLATIVE ANALYSIS OF THE ELASTIC BODY UNDER THE NONCONSERVATIVE FORCE

by

Hiroshi GOTO[I)] and Yasuhiko HANGAI[II)]

SYNOPSIS

In this paper, the Beck's problem which is a classical problem of the elastic nonconservative system is analyzed from the viewpoint of the geometrically nonlinear problem. The reduced basic nonlinear equation of motion is derived by applying the modal analysis technique to the basic equation obtained by the finite element method of the beam element. The results of the direct integration show the existance of the parametric excitative phenomenon under the load level which is much lower than the classical fluttering load level, which gradually grow up to the final stationary oscillation with the large amplitude. Paying attention to the final oscillation, the stationary oscillative analysis is performed by the harmonic balance method. Consequently, the existance of the stationary oscillative solution is proved even in the load level which is much lower than the classical fluttering load level.

INTRODUCTION

Most of the structural analysis of the elastic system which belong to either static problem or dynamic problem has been assumed to be subject to some conservative load. However, some problem of the elastic system belongs to the nonconservative one, for example pipes conveying fluids, nozzles spauting a rappid flow, aerofoils under high speed flight, towers under wind loads, etc., and still more, in the strict sense, most of the elastic problem may be reduced to nonconservative one. Dealing with the problem of this kind, we cannot use the energy principle or, that is to say, any variational methods based on the energy principle, and the basic differential equations derived from any virtual work prin-

---

I) Research Associate, II) Associate Professor, Institute of Industrial Science, University of Tokyo

ciples lead to the non-selfadjoint differential equations. However, we have some tools, though they are approximations, to solve the problem of this type, for example the weighted residual method, the finite difference method or the adjoint variational method which is an application of the adjoint differential system.

Modeling the problem to be analyzed, there is a typical and classical problem what is called Beck's problem. It is a problem of the beam having one clamped end and the other free end which is subject to the tangential concentrated load, as shown in Fig.1. It has been treated by many researchers as M.Beck and, H.Leipholz, V.V.Bolotin, H.Ziegler et al. and it is clarified that some peculiar facts exist as represented by the destabilizing phenomena. Actually the results of researches of this field have been already used in many branches of the mechanical engineering.

However, all of the preceding researches are based on the method of discrimination for the structural stability in which the basic equations are reduced to the complex eigenvalue problem connected with the frequency parameter, assuming the deflection of interest to be the exponential function of the time. That is to say, the system is stable if the amplitude of the deflections of the system continues to maitain some suppressed magnitude as the time parameter increases and unstable if it increases conversely. In the latter case, it is called as the flutter instability phenomenon.

Recently, the authors obtained, however, the eccentric results for the preceding Beck's problem. Namely, there exist two noteworthy phenomena, that is, first, the system with the geometrical nonlinearity become unstable in the load level which is much lower than the classical flutter instability point and second, the unstable oscillations gradually grow up to the final stationary oscillation with the large amplitude such as the van der Pole's limit cycle. These results are obtained by the direct integration method applying to the 4 degrees-of-freedom reduced system that is derived from 10 beam finite elements approximation. Introducting the load parameter λ which is based on the Euler's buckling load level $Pe(=\pi^2EJ/4l^2)$, the classical flutter load level corresponds to $\lambda \fallingdotseq 8.19$. The authors found that the preceding excitative phenomenon exists at the load level $\lambda=8.0$ and still more it exists even at the load level $\lambda=5.0$, and at each load level, the excitation ceases to the final stationary oscillation with the large amplitude. It has not only no meaning but no persuation, however possible it is, to continue to perform the simulation in order to check the existance of the excitative phenomenon at the lower load level and apart from the matter, it needs a great effort to perform the computation. Paying attention to the fact that the basic reduced equations of motion contain the stationary solution obtained by the direct integration, the

authors adopt the way to pursue the final stationary solution directly. The adopted method for this analysis is the harmonic balance method whose effective and systematic computational program has been already prepared.

Consequently, the authors obtain the result that the stationary solution exists in the region of the load level $\lambda \geq 2$ which is much less than the classical flutter load level, and there exists the so-called bifurcation phenomenon between the obtained stationary solutions.

CONSTRUCTION OF THE REDUCED BASIC EQUATIONS OF MOTION

Applying the finite element method to the Beck's rod, we adopt the beam element and devide the rod into 10 elements as shown in Fig.1. The strain-displacement relations are as follows,

$$\begin{aligned} \varepsilon &= du/ds + 1/2\{(du/ds)^2 + (dw/ds)^2\} \\ \kappa &= d^2w/ds^2 + (du/ds)(d^2w/ds^2) - (d^2u/ds^2)(dw/ds) \end{aligned} \qquad (1)$$

where ε and κ represent the axial strain and the curvature, respectively. In this representation no omission is contained without the assumption of $\varepsilon \ll 1$.

After the usual derivation of the finite element process, we obtain the basic equation of motion as the following equations.

$$[M_{ij}]\{\ddot{d}_j\} + [K_{ij}]\{d_j\} + [K_{ijk}]\{d_j\}\{d_k\} + [K_{ijkl}]\{d_j\}\{d_k\}\{d_l\} = \{P_i\} \qquad (2)$$

where $i,j,k,l = 1 \sim N$, N: Total freedom of the system
In order to enable us to grasp the essence of this problem and to treat simply, the modal analysis technique is applied to Eq.(2). Constituting the modal matrix, we introduce the linear eigenvalue problem as follows,

$$[M_{ij}]\{\ddot{d}_j\} + [K_{ij}]\{d_j\} = \{0\} \qquad i,j = 1 \sim N \qquad (3)$$

After solving Eq.(3), we select four modal vectors in which two of them correspond to the first and the second natural oscillations of the axial direction and the others of the lateral directions. Then the modal matrix is represented as follows,

$$[\overset{4}{\Phi}_{ij}] \qquad N: \text{Total freedom of the system} \qquad (4)$$

Using it, we obtain the reduced nonlinear equation of motion as the following equation.

$$\{\ddot{x}_i\} + \omega_i^2\{x_i\} + [\overset{*}{K}_{ijk}]\{x_j\}\{x_k\} + [\overset{*}{K}_{ijkl}]\{x_j\}\{x_k\}\{x_l\} = \{\overset{*}{P}_i\} \qquad (5)$$

where x_1, x_2 ; the generalized coodinate of the axial direction
x_3, x_4 ; the generalized coodinate of the lateral direction

$$\{d_r\}=[\Phi_{rj}]\{x_j\}$$
$$[K^*_{ijk}]=[K_{rst}][\Phi_{ri}][\Phi_{sj}][\Phi_{tk}]$$
$$[K^*_{ijkl}]=[K_{rstu}][\Phi_{ri}][\Phi_{sj}][\Phi_{tk}][\Phi_{ul}]$$
$$\{P^*_i\}=\{P_r\}[\Phi_{ri}] \qquad r,s,t,u=1\sim N;\ i,j,k,l=1\sim 4$$

The follower force vector acting the free end of the bar is estimated as follows,

$$\{P_i\}^T=\{0,\ldots,0,0,-\lambda N\cos\theta_n,-\lambda\sin\theta_n,0\} \tag{6}$$

where $\theta_n=\tan^{-1}d_N$

On the other hand, there is a relation between the generalized coordinates x_i and the displacement d_N as follows,

$$d_N=\sum_{j=1}^{4}\Phi_{Nj}x_j \tag{7}$$

From Eq.(6), we obtain the generalized force vector as follows,

$$\{P^*_i\}=-\lambda\{\Phi_{N-2,i}\cos\theta_n+\Phi_{N-1,i}\sin\theta_n\} \tag{8}$$

Substituting Eq.(7) into Eq.(8), the generalized force vector is represented approximately by the generalized coodinates only as follows,

$$\{P^*_i\}=-\lambda\{\Phi_{N-2,i}\cos(\sum_{j=1}^{4}\Phi_{Nj}x_j)+\Phi_{N-1,i}\sin(\sum_{j=1}^{4}\Phi_{Nj}x_j)\} \tag{9}$$

Regarding the relation $\sin\varepsilon=\varepsilon-\varepsilon^3/3!+O(\varepsilon^5)$ and $\cos\varepsilon=1-\varepsilon^2/2!+O(\varepsilon^4)$ and omitting the higher order, we obtain the generalized force vector's representation as the following equation.

$$\{P^*_i\}=\lambda(\{F^*_i\}-[E^*_{ij}]\{x_j\}-[E^*_{ijk}]\{x_j\}\{x_k\}-[E^*_{ijkl}]\{x_j\}\{x_k\}\{x_l\}) \tag{10}$$

where

$$\{F^*_i\}=-\{\Phi_{N-2,i}\}$$
$$[E^*_{ij}]=\{\Phi_{N-1,i}\}\{\Phi_{Nj}\}$$
$$[E^*_{ijk}]=-(1/2)\{\Phi_{N-2,i}\}\{\Phi_{Nj}\}\{\Phi_{Nk}\}$$
$$[E^*_{ijkl}]=-(1/6)\{\Phi_{N-1,i}\}\{\Phi_{Nj}\}\{\Phi_{Nk}\}\{\Phi_{Nl}\} \qquad i,j,k,l=1\sim 4$$

Substituting Eq.(10) into Eq.(5), we obtain the nonlinear equation of motion as follows,

$$\{\ddot{x}_i\}+([\omega^2]+\lambda[E^*_{ij}])\{x_j\}+([K^*_{ijk}]+\lambda[E^*_{ijk}])\{x_j\}\{x_k\}$$
$$+([K^*_{ijkl}]+\lambda[E^*_{ijkl}])\{x_j\}\{x_k\}\{x_l\}=\lambda\{F^*_i\} \qquad i,j,k,l=1\sim4 \qquad (11)$$

where $[\omega^2]=\begin{bmatrix}\omega_1^2 & & 0 & \\ & \omega_2^2 & & \\ & & \omega_3^2 & \\ 0 & & & \omega_4^2\end{bmatrix}$

This is the reduced nonlinear equation of motion for the Beck's problem.

THE DIRECT INTEGRATION

The results of the direct integration by the Runge-Kutta method are depicted in Fig.2. Adopted Δt for this simulation is automatically controlled in order to suppress the error due to the high frequency oscillations. Fig.2-a and Fig.2-b show the results for the case in which $\dot{x}_3=1\times10^{-3}, \dot{x}_4=0$ and $\dot{x}_3=0, \dot{x}_4=1\times10^{-3}$ are given to the system as the initial value, respectively and again, λ expresses the load parameter based on the Euler's buckling load. These results show that there is a phenomenon of the increasing of an amplitude at the load level $\lambda=7.0, 6.0$ and 5.0 which are much lower than the critical flutter load level and that this phenomenon does not depend on the initial values. Fig.3, Fig.4 and Fig.5 also show the results of the direct integration. Differing from Fig.3, these are the results of the direct integration for the long time length. From these figures, we can see the existance of the gradually converged final stationary oscillations with the large amplitude at the each load level, which are less than the classical flutter load level.

The results of the direct ingegration show that there is some divergence phenomenon surely caused by the coupling between the nonlinear terms, but there is no further data to explain the mechanism of this phenomenon. Subsequently, we try to clarify this fact by investigating the 2 degrees-of-freedom reduced system as the following section.

INVESTIGATION OF THE 2 DEGREES-OF-FREEDOM REDUCED SYSTEM

As has been stated in the preceding section, we investigate the 2 degrees-of-freedom system. In Eq.(11), estimating the generalized displacements of the axial direction x_1 and x_2 as static and linear, we obtain the 2 degrees-of-freedom nonlinear equation of motion expressed only by the lateral generalized displacements x_3 and x_4 as the following equations.

$$\{\ddot{x}_i\}+([\omega^2]+\lambda[E^*_{ij}]+2\lambda[\tilde{K}_{ij}])\{x_j\}+[K^*_{ijkl}]\{x_j\}\{x_k\}\{x_l\}=\{0\} \quad i,j=3,4 \quad (12)$$

where $[\tilde{K}_{ij}]=[K^*_{ija}]\{x_a\}$ $\quad a=1,2$

$\{x_a\}$; the axial displacements estimated staticaly and linearly

In this representation, the quadratic nonlinear terms are not contained because of properties of the coupling between the lateral displacements of the system without the geometrical curvature. Cutting off the cubic nonlinear terms of Eq.(12), we also prepare the linearized system as the following equations.

$$\{\ddot{x}_i\}+([\omega^2]+\lambda[E^*_{ij}]+2\lambda[\tilde{K}_{ij}])\{x_j\}=\{0\} \qquad i,j=3,4 \tag{13}$$

The results of the direct integration of Eq.(13) and Eq.(12) are depicted in Fig.6 and Fig.7, respectively. Fig.6 shows that there is the flutter phenomenon only in the region of $\lambda \geq 8.2$ corresponding to the classical theory and that the almost periodic oscillation occurs in the region of $\lambda < 8.2$. On the contrary, we obtain no boundlessly fluttering oscillation from Eq.(12) as shown in Fig.7 and there are only the almost periodic oscillations. As there are great differencies between the results of Eq.(11) and the results of Eq.(12) or Eq.(13), we reach the conclusion that the fundamental cause of the preceding fluttering is the existance of the oscillations of the axial direction. Consequently, we obtain the physically reasonable conclusion of the fluttering phenomenon which corresponds to the parametric excitative phenomenon.

THE STATIONARY OSCILLATIVE ANALYSIS

As has been stated, the nonlinear equation of motion (11) contains the stationary oscillative solution as shown in the results of the direct integration. Accordingly, it is rather natural to pursue the stationary solution directly for the aim of discrimination of the critical load of the system. So large as the amplitude of the stationary oscillation obtained by the direct integration is, only a few methods can be applied to the present problem for the stationary oscillative analysis. One of the numerical methods which can satisfy the requirement of the accuracy may be the harmonic balance method which can express the solution strictly in the space of the assumed functions by solving the nonlinear algebraic simultaneous equation numerically. As there is, however, no solution for the first approximation to be converged to the correct solution, we perform the frequency analysis for the final asymptotic oscillations of the results of the direct integration. The results of this analysis are shown by a histogram in Fig.8, where the wave of the generalized displacement x_3 is taken as a basic harmonic. Whereas, for example, the predominant harmonics for the load level $\lambda=6$ prove to be $\cos\omega t$, $\sin\omega t$ for x_3 and $\cos\omega t$, $\cos 3\omega t$, $\cos 5\omega t$, $\cos 7\omega t$, $\sin\omega t$, $\sin 3\omega t$, $\sin 5\omega t$, $\sin 7\omega t$ for x_4 . From these figures, we can see that the weight of the

higher frequency becomes larger as the load parameter decreases.

Consequently, it may be sufficient to take the assumed harmonics for the stationary oscillative analysis shown as follows,

$$
\begin{aligned}
x_1 &= c_{10} + c_{12}\cos 2\omega t \\
x_2 &= c_{20} + c_{22}\cos 2\omega t \\
x_3 &= c_{31}\cos\omega t + s_{31}\sin\omega t \\
x_4 &= c_{41}\cos\omega t + c_{43}\cos 3\omega t + c_{45}\cos 5\omega t + s_{41}\sin\omega t + s_{43}\sin 3\omega t + s_{45}\sin 5\omega t
\end{aligned}
\tag{14}
$$

where $c_{10}, c_{12}, c_{20}, c_{22}, c_{31}, s_{31}, c_{41}, c_{43}, c_{45}, s_{41}, s_{43}, s_{45}$ are the unknown variables to be calculated by the harmonic balance analysis and the successive analysis of the nonlinear algebraic simultaneous equations. Applying the assumed harmonics to the basic nonlinear equation of motion (11), we obtain the nonlinear algebraic simultaneous equation as follows,

$$
[A_{ij}]\{c_j\} + [A_{ijk}]\{c_j\}\{c_k\} + [A_{ijkl}]\{c_j\}\{c_k\}\{c_l\} = \{f_i\} \quad i,j,k,l = 1 \sim 12 \tag{15}
$$

where $\{c_i\}^T = \{c_{10}, c_{12}, c_{20}, c_{22}, c_{31}, s_{31}, c_{41}, c_{43}, c_{45}, s_{41}, s_{43}, s_{45}\}$

Adopting the results of the preceding frequency analysis as first approximate solutions and applying the arc-length method for Eq. (15), we readily obtain the converged solutions. The results of this analysis are graphically depicted in Fig.9, and the change of the unknown variables is depicted in Fig.10-1 ~ Fig.10-3. And the maximum amplitudes of the generalized displacements x_3 and x_4 are depicted in Fig.11. The λ-ω curve is shown in Fig.12. In these figures, there seems to be a singular point near the load level $\lambda = 4.1$. Actually, solving the nonlinear algebraic simultaneous equation (15) from the higher load level to the lower one, one cannot obtain the equilibrium path continuously. If one continue to perform the preceding process, however possible it is, the results obtained in the region of $\lambda < 4.1$ prove to be a meaningless solution from the viewpoint of the practical questions, because these results become clear to be the unstable solutions from the stability analysis. Consequently, it is necessary to perform to calculate by the bifurcation technique to obtain the further equilibrium path.

This bifurcation phenomenon is supported by the results of the preceding direct integration. The result of the direct integration for the load level $\lambda = 8.0$ is depicted in Fig.13. From this figure, one can see that the oscillations of the generalized displacements x_3 and x_4 grow up together without the phase difference to some extent and that in the bifurcation range in the

diagram where the amplitudes of them grow up to some magnitude, the descrepancy of the phase suddenly occurs, which may be a trigger of the increase of the amplitudes of x_3 and x_4 . This qualitative explanation can be made for any cases of the load level as shown in Fig.14 and is also supported by the results of the harmonic balance analysis. Namely, there is an unstable solution on the extention of the equilibrium path of the load level $2<\lambda<4$ in the extent of the load level $\lambda > 4$, which is depicted in Fig.11 as a broken line. The initially disturbed system firstly increases its amplitude gradualy up to the level described by a broken line, where the system pauses to increase its amplitude for a while and secondly, after the bifurcation phenomenon, the system starts to grow up to the final stationary oscillation of the large amplitude.

CONCLUDING REMARK

It is proved that the stationary oscillative solution of the Beck's problem with the nonlinearity exists in the comprehensive range of the load level even in the load level which is much lower than the critical flutter load level of the classical theory. This results is supported not only by the simple direct integration but also by the stationary oscillative analysis in which two results completely coincide together. Furthermore, the stationary oscillative solution with the large amplitude exists even in the load level $\lambda=2$. These results imply that the critical load level of the Beck's problem exist at least in the load level lower than $\lambda=2$ from the viewpoint of the nonlinear oscillative analysis, which is more actual treatment than the linear eigenvalue analysis. What is more important, it can be expected especially from the result of the stationary oscillative analysis that the critical load level of the Beck's problem approaches the Euler's buckling load level gradually, though the converged solutions are not obtained in the lower region than $\lambda=2$, probably because of the lack of the assumed harmonics.

REFERENCES

[1] Beck,M., ZAMP, Vol.3(1952), p.225.
[2] Leipholz,H., Stability Theory, Academic Press(1970).
[3] Bolotin,V.V., Nonconservative Problems of the Theory of Elastic Stability, Pergomon Press(1963).
[4] Ziegler,H., Principles of Structural Stability, Blaisdell(1968).
[5] Minakawa,Y., Doctor's thesis, University of Tokyo(1976).
[6] Goto,H. and Hangai,Y., Bulletin of ERS, No.10(1976), p.48.
[7] Goto,H. and Hangai,Y., Proc. of the Annual Convention of AIJ(1978), p.1005.

(Manuscript was received on January 22, 1980)

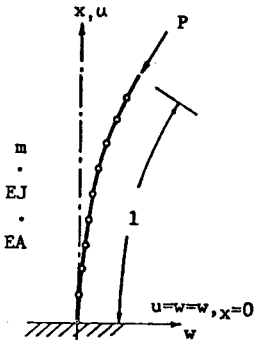

P=λ·Pe

λ : Load Parameter

Pe: Euler's Buckling Load

m : Mass per unit length

EJ: Bending Stiffness

A : Section area

1 : Length of Rod

Fig.1 Beck's rod

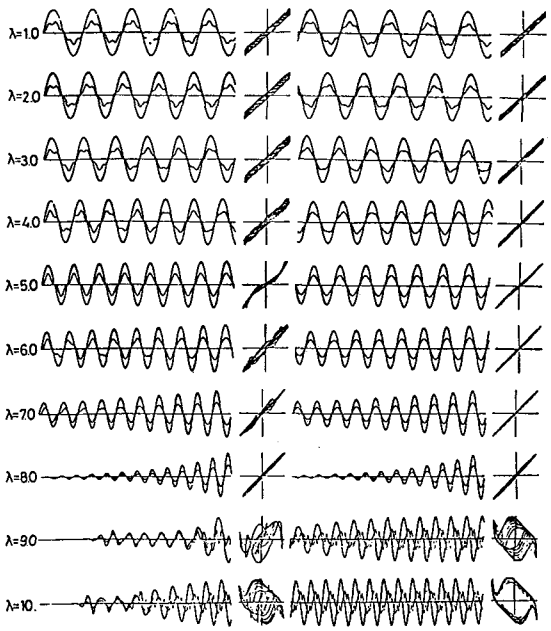

Fig.2-a Results of the direct integration of the 4 degrees-of-freedom system and the X3-X4 phase plane ($\dot{X}3=1.0\times10^{-3}$, $\dot{X}4=0.0$)

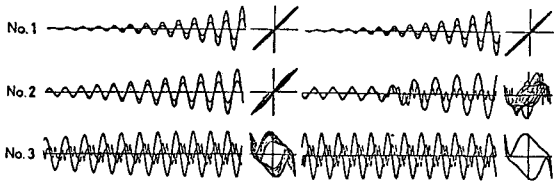

Fig.3 Results of the direct integration of the 4 degrees-of-freedom system and the X3-X4 phase plane ($\lambda=8$, $\dot{X}3=1\times10^{-3}$, $\dot{X}4=0$)

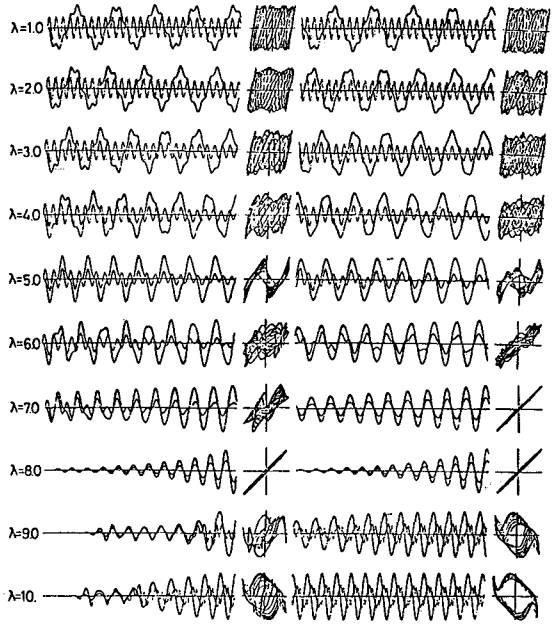

Fig2-b Results of the direct integration of the 4 degrees-of-freedom system and the X3-X4 phase plane ($\dot{X}3=0$, $\dot{X}4=1\times10^{-3}$)

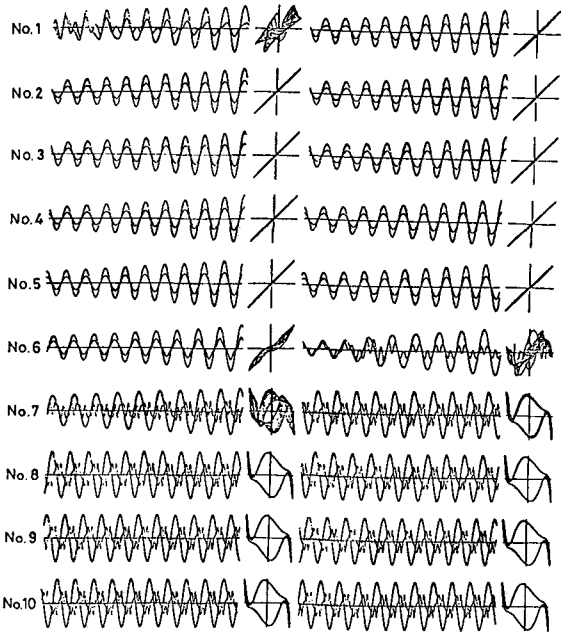

Fig.4 Results of the direct integration of the 4 degrees-of-freedom system and the X3-X4 phase plane ($\lambda=7$, $\dot{X}3=1\times10^{-3}$, $\dot{X}4=0$)

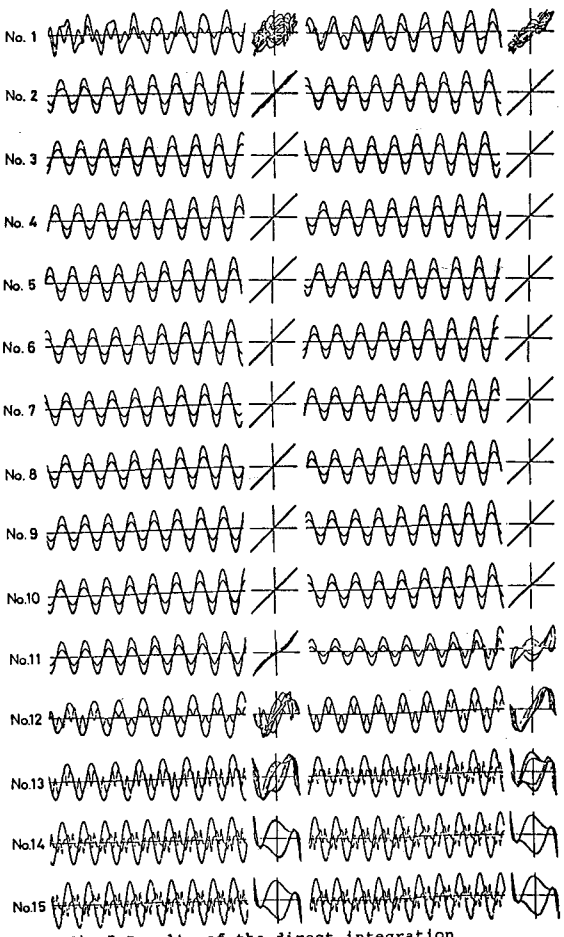

Fig.5 Results of the direct integration of the 4 degrees-of-freedom system and the X3-X4 phase plane ($\lambda=6, \dot{X}3=1\times10^{-3}, \dot{X}4=0$)

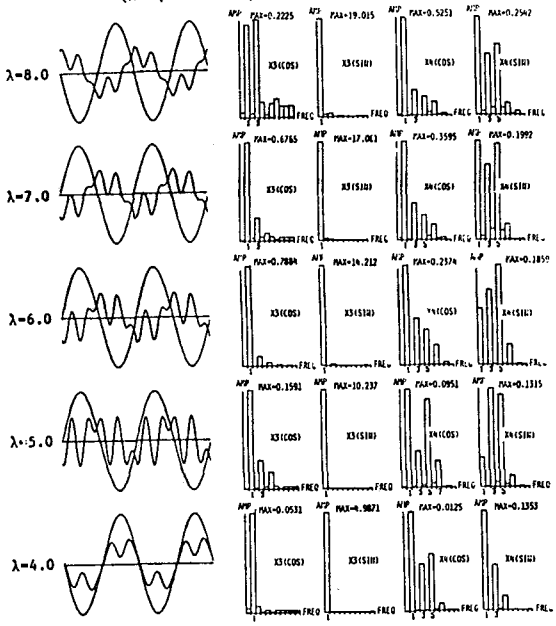

Fig.8 Results of the frequency analysis

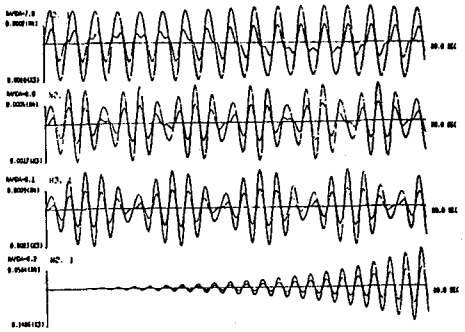

Fig.6 Results of the direct integration of the 2 degrees-of-freedom linear system ($\dot{X}3=1\times10^{-3}, \dot{X}4=0$)

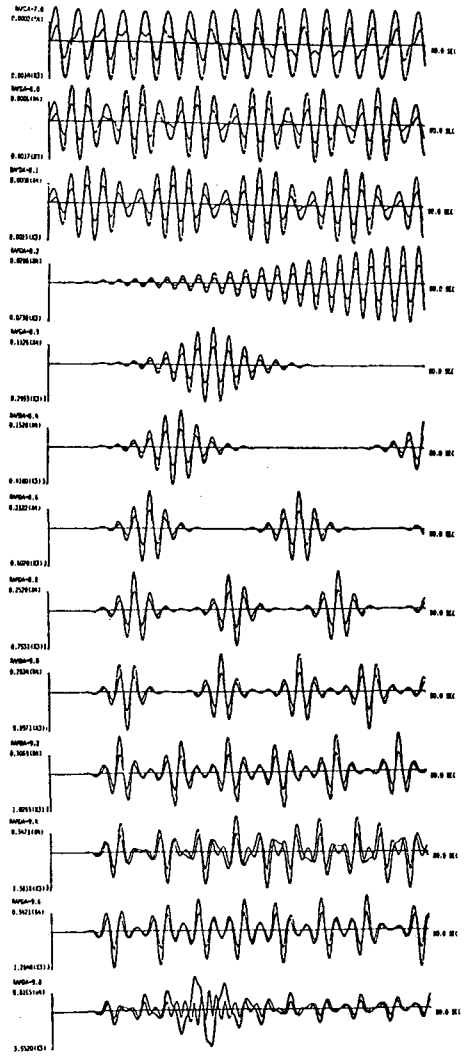

Fig.7 Results of the direct integration of the 2 degrees-of-freedom nonlinear system ($\dot{X}3=1\times10^{-3}, \dot{X}4=0$)

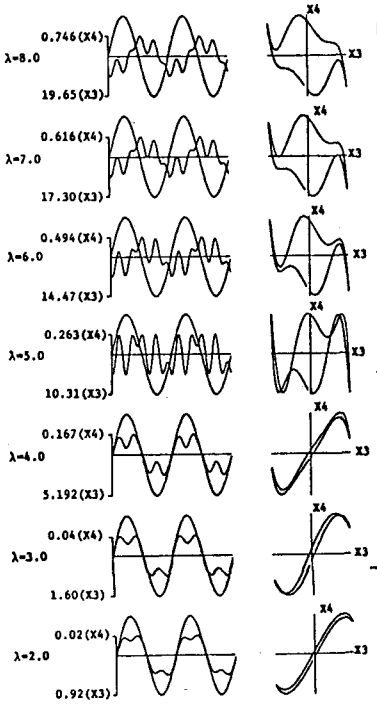

Fig.9 Results of the harmonic balance method (12 waves approximation)

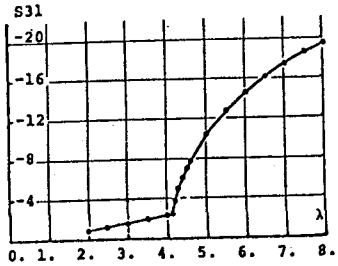

Fig.10-1 S31-λ curve

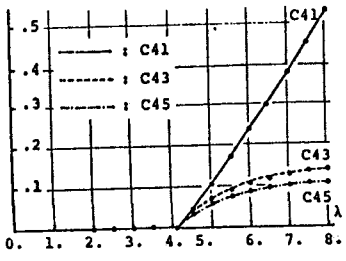

Fig.10-2 C41,C43,C45-λ curves

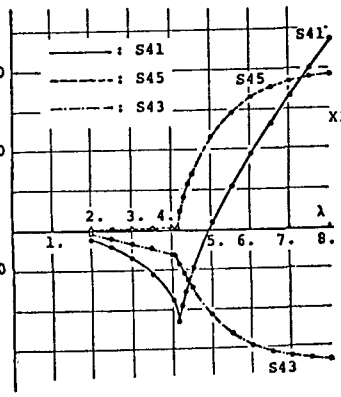

Fig.10-3 S41,S43,S45-λ curves

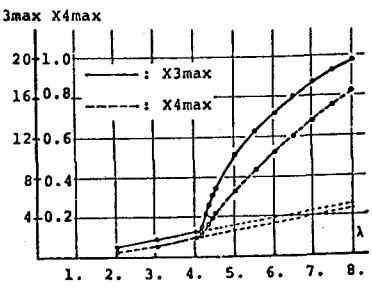

Fig.11 X3max,X4max-λ curves

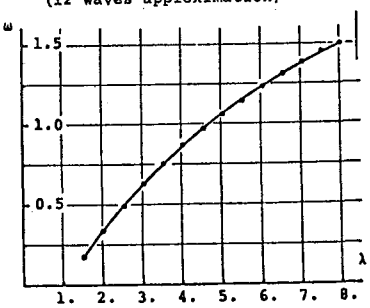

Fi.12 λ-ω curve

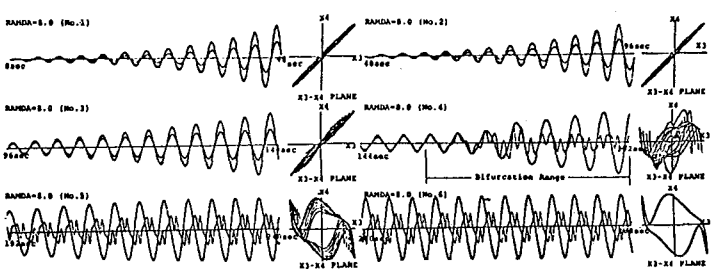

Fig.13 Bifurcation range (λ=8)

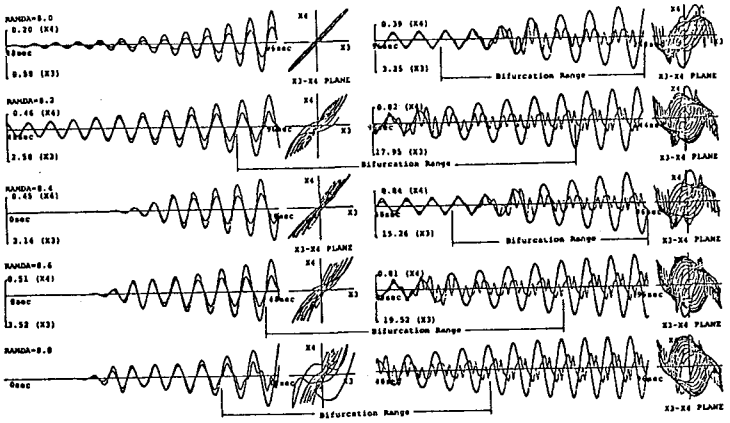

Fig.14 Bifurcation range (λ=8.0,8.2,8.4,8.6,8.8)